

Glauber theory of initial- and final-state interactions in $(p, 2p)$ scattering

O.Benhar¹, S.Fantoni^{2,3}, N.N.Nikolaev^{4,5}, J.Speth⁴, A.A.Usmani², B.G.Zakharov⁵

¹*INFN, Sezione Sanità, Physics Laboratory, Istituto Superiore di Sanità. I-00161 Roma, Italy*

²*Interdisciplinary Laboratory, SISSA, INFN, Sezione di Trieste. I-34014, Trieste, Italy*

³*International Centre for Theoretical Physics, Strada Costiera 11, I-34014, Trieste, Italy*

⁴*IKP(Theorie), Forschungszentrum Jülich GmbH.*

D-52425 Jülich, Germany

⁵*L.D.Landau Institute for Theoretical Physics,*

GSP-1, 117940, ul.Kosygina 2., V-334 Moscow, Russia

(February 21, 2018)

Abstract

We develop the Glauber theory description of initial- and final-state interactions (IFSI) in quasielastic $A(p, 2p)$ scattering. We study the IFSI-distortion effects both for the inclusive and exclusive conditions. In inclusive reaction the important new effect is an interaction between the two sets of the trajectories which enter the calculation of IFSI-distorted one-body density matrix for inclusive $(p, 2p)$ scattering and are connected with incoherent elastic rescatterings of the initial and final protons on spectator nucleons. We demonstrate that IFSI-distortions of the missing momentum distribution are large over the whole range of missing momentum both for inclusive and exclusive reactions and affect in a crucial way the interpretation of the BNL data on $(p, 2p)$ scattering. Our numerical results show that

in the region of missing momentum $p_m \lesssim 100 - 150$ MeV/c the incoherent IFSI increase nuclear transparency by 5-10%. The incoherent IFSI become dominant at $p_m \gtrsim 200$ MeV/c.

I. INTRODUCTION

The strength of the initial- and final-state interactions (IFSI) in $(p, 2p)$ scattering is usually characterized by the nuclear transparency, T_A , defined as a ratio of the experimentally measured cross section to the theoretical cross section calculated neglecting IFSI in the plane wave impulse approximation (PWIA). It is expected that, due to the color transparency (CT) phenomenon [1,2], IFSI effects will vanish and the nuclear transparency will tend to unity in $(p, 2p)$ reaction in the limit of $s \rightarrow \infty$ and $|t|/s \sim 1$. From the point of view of the Glauber-Gribov coupled-channel multiple scattering theory [3,4] the vanishing of IFSI corresponds to a cancellation of the rescattering amplitudes with elastic (diagonal) and excited (off-diagonal) intermediate states of the initial and final protons participating in hard pp scattering. Naive theoretical considerations [1,2] suggest a monotonic rise of T_A with s in the case of dominance of the point-like perturbative mechanism of hard pp scattering [5]. However, in the BNL experiment [6] on large-angle $(p, 2p)$ scattering at the beam momenta 6-12 GeV/c near $\theta_{c.m.} = 90^\circ$ (here $\theta_{c.m.}$ is the scattering angle in the pp center of mass frame) a decrease of T_A was observed at beam momenta $\gtrsim 10$ GeV/c. There were suggestions [7-9] that the irregular behavior of T_A is due to an interplay of CT effects for hard point-like and non-point-like, resonance or Landshoff, mechanisms of large-angle pp scattering. None the less, from our point of view, a satisfactory explanation was not found, and up to now the theoretical situation is far from being clear.

In previous works on CT effects in $(p, 2p)$ reaction the IFSI-absorption effects were treated within the optical potential approach. This approximation corresponds to taking into account only the coherent IFSI. In this case the calculated cross section is related to the exclusive $(p, 2p)$ reaction, when the final states of the residual nucleus are exhausted by the one-hole excitations of the target nucleus. The allowance for both the coherent and incoherent IFSI corresponds to the inclusive reaction, when all the final states of the residual nucleus are involved. The recent Glauber analysis [10] indicates that in the case of $(e, e'p)$ scattering the incoherent rescatterings become dominant at high missing momenta ($\gtrsim 250$

MeV/c). Evidently, in $(p, 2p)$ scattering, due to the increase of the number of the fast protons propagating through the nuclear medium as compared with $(e, e'p)$ reaction, the relative effect of the incoherent rescatterings will be enhanced. The theoretical study of the inclusive reaction would be of great importance because the data of the BNL experiment [6] correspond namely to the inclusive conditions. The analysis of the missing momentum dependence of the nuclear transparency in $(p, 2p)$ reaction within the coupled-channel formalism including the incoherent rescatterings invites complications. First, evaluation of the contribution of the off-diagonal incoherent rescatterings requires information on the off-diagonal resonance-nucleon amplitudes at arbitrary momentum transfer [11,12]. Second, inclusion of the incoherent rescatterings make the coupled-channel analysis complicated from the point of view of the numerical computations. In this situation it is reasonable to start the study of IFSI effects in hard $(p, 2p)$ reaction with inclusion of the incoherent rescatterings within the one-channel Glauber model. Evidently, only after a comparison of the experimental data with the predictions of the Glauber model one can understand whether and to which extent the off-diagonal rescatterings or other effects are really important. The Glauber analysis [10] of the missing momentum distribution in $(e, e'p)$ scattering shows that there is a region of the relatively small missing momenta ($p_m \lesssim 150$ MeV/c) where the incoherent rescatterings can be neglected. This fact allows one to greatly simplify evaluation of CT effects in this region of the missing momentum [12]. From the point of view of further investigations of CT effects in $(p, 2p)$ scattering it is of great importance to clarify whether this is the case in this reaction as well. For the above reasons the Glauber analysis of $(p, 2p)$ scattering is highly desirable. In the current literature only in ref. [13] the Glauber formalism was applied for evaluation of the nuclear transparency in inclusive $(p, 2p)$ reaction. However, unjustified approximations made in ref. [13] led to a loss of the IFSI-distortion effects (for the criticism of the approach [13] see ref. [10] and the discussion in section 2 of the present paper).

In the present paper we evaluate the nuclear transparency in $(p, 2p)$ scattering within the Glauber model in the region of $p_m \lesssim 300$ MeV/c. In our analysis we neglect the short

range correlations (SRC) in the target nucleus and describe the nucleus wave function within independent particle shell model. In the case of the single particle momentum distribution (SPMD) the effects of SRC [14] are still marginal in this region of momenta. The analysis of $(e, e'p)$ [15,16] shows that at $p_m \lesssim 300$ MeV/c SRC practically do not affect the missing momentum dependence of the nuclear transparency as well. In $(p, 2p)$ reaction the distortion effects are enhanced as compared to the case of $(e, e'p)$ scattering. It improves the credibility of the independent particle shell model for analysis of $(p, 2p)$ scattering as compared to the case of $(e, e'p)$ reaction.

In our analysis, as in previous works on hard $(p, 2p)$ reaction, we assume the factorization of hard pp scattering and soft IFSI. We are fully aware that due to the strong energy dependence of the cross section of hard pp scattering ($\propto s^{-10}$) this approximation may be questionable. The qualitative estimates show that the off-shell effects and the nonzero energy momentum transfer in soft IFSI in the kinematical region of our interest can increase the nuclear transparency by 20-50%. Unfortunately a rigorous evaluation of these effects, requiring the relativistic many body approach to the $(p, 2p)$ reaction, is not possible at present. However, as we will see the IFSI-distortion effects are typically much stronger than the expected magnitude of effects connected with the off-shellness of the bound proton and the energy transfer in soft IFSI. Therefore, we believe that the factorized approximation for hard pp scattering and soft IFSI is a good starting point for evaluation of the IFSI-distortion effects in hard $(p, 2p)$ reaction.

The paper is organized as follows. In section 2 we set out the Glauber formalism for hard $(p, 2p)$ reaction. The numerical results are presented in section 3. In this section we also compare the predictions of the Glauber model with the data on the nuclear transparency and the missing momentum distribution obtained in the BNL experiment [6,17]. The summary and conclusions are presented in section 4.

II. IFSI IN $(p, 2p)$ SCATTERING WITHIN THE GLAUBER FORMALISM

We begin with the kinematics of hard $(p, 2p)$ reaction. We denote the four momenta of the initial and two final protons participating in hard pp scattering as (E_1, \vec{p}_1) and (E_3, \vec{p}_3) , (E_4, \vec{p}_4) respectively. The trajectories of the initial and final protons will be also labeled by indexes 1 and 3,4. We use the coordinate system with z -axis along \vec{p}_1 and the x -axis in the reaction plane. At high energy for $\theta_{c.m.} = 90^\circ$ the angle between the three momenta of the final protons and z -axis in the laboratory frame, $\theta_{l.f.}$, becomes small ($\theta_{l.f.} \sim [2m_p(E_1 - m_p)]^{1/2}/E_1$, here m_p is the proton mass). Below we will make use of this fact to simplify the numerical calculations. As was stated in section 1, we assume the factorization of hard pp scattering and soft IFSI of the fast protons with spectator nucleons. Then, the differential cross section of $(p, 2p)$ scattering can be written through the distorted spectral function, $S(E_m, p_m, E_1)$, in the form

$$\frac{d^3\sigma}{dt dE_m d\vec{p}_m^3}(E_1, t, E_m, \vec{p}_m) = \frac{d\sigma_{pp}}{dt}(s, t) S(E_m, \vec{p}_m, E_1), \quad (1)$$

where $d\sigma_{pp}/dt$ is the differential cross section of hard pp scattering, the missing momentum and missing energy are defined as $\vec{p}_m = \vec{p}_3 + \vec{p}_4 - \vec{p}_1$, $E_m = E_3 + E_4 - E_1$, s is the center of mass energy squared of the pp system. To leading order in the missing momentum s is given by

$$s \approx s_0 \left(1 - \frac{p_{m,z}}{m_p} \right), \quad (2)$$

where $s_0 = 2m_p(E_1 + m_p)$. Notice that keeping in Eq. (2) the second order terms in \vec{p}_m does not make much sense because the energy momentum transfer in the soft rescatterings of the fast initial and final protons in the nuclear medium, which is neglected in the factorized approximation (1), also gives the effect of the second order in \vec{p}_m . As was mentioned in section 1, an accurate treatment of such effects, and of the off-shell effects, requires making use of the relativistic many body approach, which goes beyond the scope of our exploratory study.

The distorted spectral function, which, under the factorized approximation (1), accumulates all the IFSI effects, can be written as

$$S(E_m, \vec{p}_m) = \sum_f |M_f(\vec{p}_m)|^2 \delta(E_m + E_{A-1}(\vec{p}_m) - m_A), \quad (3)$$

where $M_f(\vec{p}_m)$ is the reduced matrix element of the exclusive process $p + A_i \rightarrow p + p + (A-1)_f$. In Eq. (3) and hereafter for the sake of brevity the variable E_1 is suppressed. In the present paper we will study IFSI-distortion effects at the level of the missing momentum distribution, $w(\vec{p}_m)$, which reads

$$w(\vec{p}_m) = \frac{1}{(2\pi)^3} \int dE_m S(E_m, \vec{p}_m). \quad (4)$$

The substitution of (3) into (4) yields

$$w(\vec{p}_m) = \frac{1}{(2\pi)^3} \sum_f |M_f(\vec{p}_m)|^2. \quad (5)$$

In our analysis we confine ourselves to a large mass number of the target nucleus $A \gg 1$. Then, neglecting the center of mass correlations we can write $M_f(\vec{p}_m)$ as

$$M_f(\vec{p}_m) = \int d^3\vec{r}_1 \dots d^3\vec{r}_A \Psi_f^*(\vec{r}_2, \dots, \vec{r}_A) \Psi_i(\vec{r}_1, \dots, \vec{r}_A) S(\vec{r}_1, \dots, \vec{r}_A) \exp(i\vec{p}_m \vec{r}_1). \quad (6)$$

Here Ψ_i and Ψ_f are wave functions of the target and residual nucleus, respectively. The nucleon "1" is chosen to be the struck proton. The use of the same indexes for the spatial coordinates of the nucleons in the nucleus wave functions and for labeling the fast protons participating in hard pp scattering must not lead to a confusion because we will not use the spatial coordinates of the fast initial and final protons. For the sake of brevity, in Eq. (6) and hereafter the spin and isospin variables are suppressed. The factor $S(\vec{r}_1, \dots, \vec{r}_A)$ in Eq. (6) takes into account the soft IFSI-distortion effects. In the Glauber model it can be written in the form

$$S(\vec{r}_1, \dots, \vec{r}_A) = S_1(\vec{r}_1, \dots, \vec{r}_A) S_3(\vec{r}_1, \dots, \vec{r}_A) S_4(\vec{r}_1, \dots, \vec{r}_A) \quad (7)$$

where $S_{1,3,4}(\vec{r}_1, \dots, \vec{r}_A)$ are the absorptive factors for the initial and final protons which are given by

$$S_i(\vec{r}_1, \dots, \vec{r}_A) = \prod_{j=2}^A [1 - \gamma_i(\vec{r}_1, \vec{r}_j)], \quad (8)$$

with

$$\gamma_i(\vec{r}_1, \vec{r}_j) = \theta(\vec{n}_i(\vec{r}_j - \vec{r}_1))\Gamma_i(b_i(\vec{r}_1, \vec{r}_j)). \quad (9)$$

Here \vec{n}_i are the unit vectors defined as $\vec{n}_1 = -\vec{p}_1/|\vec{p}_1|$ and $\vec{n}_{3,4} = \vec{p}_{3,4}/|\vec{p}_{3,4}|$, $b_i(\vec{r}_1, \vec{r}_j) = [(\vec{r}_j - \vec{r}_1)^2 - (\vec{n}_i(\vec{r}_j - \vec{r}_1))^2]^{1/2}$ is the transverse distance between the spectator nucleons "j" and the trajectory of the fast (initial or final) proton "i", Γ_i is the familiar profile function of the elastic proton-nucleon scattering (the label "i" reflects the fact that the profile function must be calculated at the energy E_i). Eqs. (7), (8) are written under the usual assumption that the spectator coordinates can be considered as frozen during propagation of the fast protons through the nuclear medium. Also, we neglect the interaction radius of 90° hard pp scattering, which is expected to be $\sim 1/\sqrt{s}$.

In our calculations we use for $\Gamma(\vec{b})$ the standard high-energy parameterization

$$\Gamma(b) = \frac{\sigma_{tot}(pN)(1 - i\alpha_{pN})}{4\pi B_{pN}} \exp\left[-\frac{b^2}{2B_{pN}}\right]. \quad (10)$$

Here α_{pN} is the ratio of the real to imaginary part of the forward elastic pN amplitude, B_{pN} is the diffractive slope describing the t dependence of the elastic proton-nucleon cross section

$$\frac{d\sigma_{el}(pN)}{dt} = \frac{d\sigma_{el}(pN)}{dt}\Big|_{t=0} \exp(-B_{pN}|t|). \quad (11)$$

After substituting expression (6) into Eq. (5) and making use of the closure relation

$$\sum_f \Psi_f(\vec{r}'_2, \dots, \vec{r}'_A)\Psi_f^*(\vec{r}_2, \dots, \vec{r}_A) = \prod_{j=2}^A \delta(\vec{r}'_j - \vec{r}_j) \quad (12)$$

to sum over all the final states of the residual nucleus, we can represent $w(\vec{p}_m)$ in the form

$$w(\vec{p}_m) = \frac{1}{(2\pi)^3} \int d^3\vec{r}_1 d^3\vec{r}'_1 \rho_D(\vec{r}_1, \vec{r}'_1) \exp[i\vec{p}_m(\vec{r}_1 - \vec{r}'_1)], \quad (13)$$

where

$$\rho_D(\vec{r}_1, \vec{r}'_1) = \int \prod_{j=2}^A d^3\vec{r}_j \Psi_i(\vec{r}_1, \vec{r}_2, \dots, \vec{r}_A)\Psi_i^*(\vec{r}'_1, \vec{r}_2, \dots, \vec{r}_A)S(\vec{r}_1, \vec{r}_2, \dots, \vec{r}_A)S^*(\vec{r}'_1, \vec{r}_2, \dots, \vec{r}_A). \quad (14)$$

The function $\rho_D(\vec{r}_1, \vec{r}'_1)$ may be viewed as an IFSI-modified one-body proton density matrix. In the PWIA, when the IFSI factors in the right-hand side of Eq. (14) equal unity, it reduces to the formula for the usual one-body proton density matrix $\rho(\vec{r}_1, \vec{r}'_1)$, and Eq. (13) reduces to the expression for SPMD

$$n_F(\vec{p}_m) = \frac{1}{(2\pi)^3} \int d\vec{r}_1 d\vec{r}'_1 \rho(\vec{r}_1, \vec{r}'_1) \exp \left[i\vec{p}_m(\vec{r}_1 - \vec{r}'_1) \right]. \quad (15)$$

As was stated in section 1, we will describe the target nucleus in the independent particle shell model. After neglecting the SRC the A -body semidiagonal density matrix $\Psi_i(\vec{r}_1, \vec{r}_2, \dots, \vec{r}_A) \Psi_i^*(\vec{r}'_1, \vec{r}'_2, \dots, \vec{r}'_A)$ still contains the Fermi correlations. To carry out the integration over the coordinates of the spectator nucleons in Eq. (14) we neglect the Fermi correlations and replace the A -body semidiagonal density matrix by the factorized form

$$\Psi_i(\vec{r}_1, \vec{r}_2, \dots, \vec{r}_A) \Psi_i^*(\vec{r}'_1, \vec{r}'_2, \dots, \vec{r}'_A) \rightarrow \rho(\vec{r}_1, \vec{r}'_1) \prod_{i=2}^A \rho(\vec{r}_i). \quad (16)$$

Here

$$\rho(\vec{r}_1, \vec{r}'_1) = \frac{1}{Z} \sum_n \phi_n^*(\vec{r}'_1) \phi_n(\vec{r}_1)$$

is the shell model one-body proton density matrix and ϕ_n are the shell model wave functions, $\rho_A(\vec{r})$ is the normalized to unity nucleon nuclear density. The errors connected with ignoring the Fermi correlations must be small because the ratio between the Fermi correlation length $l_F \sim 3/k_F$ and the interaction length corresponding to the interaction of the fast initial and final protons with the Fermi correlated spectator nucleons $l_{int} \sim 4(\sigma_{tot}(pN)\langle n_A \rangle)^{-1}$ (here $\langle n_A \rangle$ is the average nucleon nuclear density) is a small quantity (~ 0.25). Recall, that a high accuracy of the factored approximation for the many-body nuclear density in the calculation of the Glauber model attenuation factor for the small angle hadron-nucleus scattering is well known for a long time (for an extensive review on hA scattering see [18]).

After making use of the replacement (16) in Eq. (14) the missing momentum distribution (13) can be written as follows

$$w(\vec{p}_m) = \frac{1}{(2\pi)^3} \int d^3\vec{r}_1 d^3\vec{r}'_1 \rho(\vec{r}_1, \vec{r}'_1) \Phi(\vec{r}_1, \vec{r}'_1) \exp[i\vec{p}_m(\vec{r}_1 - \vec{r}'_1)], \quad (17)$$

where the IFSI factor $\Phi(\vec{r}_1, \vec{r}'_1)$ is given by

$$\begin{aligned} \Phi(\vec{r}_1, \vec{r}'_1) &= \int \prod_{j=2}^A \rho_A(\vec{r}_j) d^3\vec{r}_j S(\vec{r}_1, \vec{r}_2, \dots, \vec{r}_A) S^*(\vec{r}'_1, \vec{r}_2, \dots, \vec{r}_A) \\ &= \left[\int d^3\vec{r} \rho_A(\vec{r}) P(\vec{r}_1, \vec{r}'_1, \vec{r}) \right]^{A-1}, \end{aligned} \quad (18)$$

with

$$\begin{aligned} P(\vec{r}_1, \vec{r}'_1, \vec{r}) &= [1 - \gamma_1(\vec{r}_1, \vec{r})][1 - \gamma_3(\vec{r}_1, \vec{r})][1 - \gamma_4(\vec{r}_1, \vec{r})] \\ &\times [1 - \gamma_1^*(\vec{r}'_1, \vec{r})][1 - \gamma_3^*(\vec{r}'_1, \vec{r})][1 - \gamma_4^*(\vec{r}'_1, \vec{r})]. \end{aligned} \quad (19)$$

The right-hand side of Eq. (19) contains the terms up to sixth order in the profile functions. To simplify the calculations we neglect the terms which contain the products $\gamma_1(\vec{r}_1, \vec{r})\gamma_{3,4}(\vec{r}_1, \vec{r})$ and $\gamma_1^*(\vec{r}'_1, \vec{r})\gamma_{3,4}^*(\vec{r}'_1, \vec{r})$. Such terms correspond to simultaneous interactions of the spectator nucleon with the initial and final protons. Due to the above mentioned smallness of the scattering angle for hard pp reaction in the laboratory frame (at $p_1 \sim 10$ GeV/c $\theta_{l.f.} \sim 25^\circ$) they are only important in a narrow vicinity of the spectator position \vec{r} with the longitudinal extension considerably smaller than the interaction length of fast protons in the nuclear medium. For this reason these terms can be safely neglected in calculating the IFSI factor (18). It is also worth noting that a rigorous treatment of such effects requires taking into account the quark content of the proton and can not be performed within the Glauber model.

After neglecting the simultaneous interactions of the spectators with the initial and final protons the IFSI factor $\Phi(\vec{r}_1, \vec{r}'_1)$ can be written in the form

$$\begin{aligned} \Phi(\vec{r}_1, \vec{r}'_1) &= \left\{ 1 + \frac{1}{A} \left[\sum_{i=1,3,4} G_i(\vec{r}_1) + \sum_{i=1,3,4} G_i^*(\vec{r}'_1) + G_{34}(\vec{r}_1) + G^{34}(\vec{r}'_1) \right. \right. \\ &+ \left. \left. \sum_{i,j=1,3,4} G_i^j(\vec{r}_1, \vec{r}'_1) + \sum_{i=1,3,4} G_{34}^i(\vec{r}_1, \vec{r}'_1) + \sum_{i=1,3,4} G_i^{34}(\vec{r}_1, \vec{r}'_1) + G_{34}^{34}(\vec{r}_1, \vec{r}'_1) \right] \right\}^{A-1}, \end{aligned} \quad (20)$$

where

$$\begin{aligned}
G_{i_1, \dots, i_n}^{j_1, \dots, j_m}(\vec{r}_1, \vec{r}'_1) &= (-1)^{n+m} \int d^3\vec{r} n_A(\vec{r}) \gamma_{i_1}(\vec{r}_1, \vec{r}) \dots \gamma_{i_n}(\vec{r}_1, \vec{r}) \gamma_{j_1}^*(\vec{r}'_1, \vec{r}) \dots \gamma_{j_m}^*(\vec{r}'_1, \vec{r}) \\
&= (-1)^{n+m} \int d^3\vec{r} n_A(\vec{r}) \theta(\vec{n}_{i_1}(\vec{r} - \vec{r}_1)) \dots \theta(\vec{n}_{i_n}(\vec{r} - \vec{r}_1)) \theta(\vec{n}_{j_1}(\vec{r} - \vec{r}'_1)) \dots \theta(\vec{n}_{j_m}(\vec{r} - \vec{r}'_1)) \\
&\quad \times \Gamma_{i_1}(b_{i_1}(\vec{r}_1, \vec{r})) \dots \Gamma_{i_n}(b_{i_n}(\vec{r}_1, \vec{r})) \Gamma_{j_1}^*(b_{j_1}(\vec{r}'_1, \vec{r})) \dots \Gamma_{j_m}^*(b_{j_m}(\vec{r}'_1, \vec{r})) \quad (21)
\end{aligned}$$

(here $n_A(\vec{r}) = A\rho_A(\vec{r})$ is the nuclear density).

The IFSI factor (20) corresponds to the inclusive $(p, 2p)$ reaction, when all the final states of the residual nucleus are allowed. In a similar way, starting from the matrix element (6) and taking into account in the sum over the final states of the residual nucleus in Eq. (5) only the one-hole excitations of the target nucleus, one can obtain the coherent IFSI factor for the exclusive reaction

$$\Phi_{coh}(\vec{r}_1, \vec{r}'_1) = S_{coh}(\vec{r}_1) S_{coh}^*(\vec{r}'_1), \quad (22)$$

where

$$S_{coh}(\vec{r}_1) = \left\{ 1 + \frac{1}{A} \left[\sum_{i=1,3,4} G_i(\vec{r}_1) + G_{34}(\vec{r}_1) \right] \right\}^{A-1}. \quad (23)$$

The factorized form of $\Phi_{coh}(\vec{r}_1, \vec{r}'_1)$ allows one to write the missing momentum distribution for exclusive reaction, which we will refer to as $w_{exc}(\vec{p}_m)$, as a sum of the IFSI-distorted distributions for the one-hole excitations

$$w_{exc}(\vec{p}_m) = \frac{1}{Z} \sum_n \left| \int d^3\vec{r}_1 \phi_n(\vec{r}_1) \exp(i\vec{p}_m \vec{r}_1) S_{coh}(\vec{r}_1) \right|^2. \quad (24)$$

The terms G_i in (23) describe the usual attenuation of the initial and final protons in the nuclear medium, while the term G_{34} is related to the shadowing effect in the system of the final protons. It is connected with the rescatterings of the protons "3" and "4" on the same spectator nucleon. The transverse separation of the trajectories "3" and "4" is $\sim 2\theta_{l.f.}(z - z_1)$ (here z is the longitudinal coordinate of the spectator nucleon). Hence, the simultaneous interaction of the spectator nucleon with both fast final protons is possible up to the longitudinal distance $\sim R_{int}/\theta_{l.f.}$ (here $R_{int} = \sqrt{2B(pN)} \approx 0.8 \text{ fm}$ is the interaction radius for soft pN -scattering) from the hard collision vertex. At incident beam momentum $\sim 10 \text{ GeV}/c$ this size becomes as large as the absorption length for the

final protons in the nuclear medium. None the less, as we will see in the energy region of the BNL experiment [6] the shadowing correction to the nuclear transparency turns out to be relatively small.

Let us turn to the whole IFSI factor (20). The difference between $\Phi(\vec{r}_1, \vec{r}'_1)$ and $\Phi_{coh}(\vec{r}_1, \vec{r}'_1)$ is connected with the soft incoherent rescatterings of the fast initial and final protons in the nuclear medium. The emergence of the interference terms, like G_i^j with $i \neq j$, and of the shadowing terms G_{34}^i , G_i^{34} and G_{34}^{34} in Eq. (20) shows that the process of excitation of the residual nucleus can not be considered as a simple superposition of the effects produced by the initial and final protons. It makes impossible a probabilistic interpretation of the incoherent IFSI. The incoherent rescatterings make the IFSI factor (20) a nonfactorized function of \vec{r}_1 and \vec{r}'_1 . To leading order in $1/A$ the nonfactorized form of the IFSI factor for inclusive reaction is connected with an interaction between the two sets of the trajectories (originating from \vec{r}_1 and \vec{r}'_1) generated by the overlapping of the functions $\gamma_i(\vec{r}_1, \vec{r})$ and $\gamma_j^*(\vec{r}'_1, \vec{r})$ in the integral (21) for G -functions with $i_n, j_m \geq 1$. Due to the fast decrease of the profile function at $b \gtrsim R_{int}$, the integral (21), and the interaction between the two sets of the trajectories, vanishes unless there is a region where \vec{r} is close to all the trajectories simultaneously which emerge in (21) through the functions $\gamma_i(\vec{r}_1, \vec{r})$ and $\gamma_j^*(\vec{r}'_1, \vec{r})$. Simple geometrical consideration shows that the interaction between the two sets of the trajectories generated by the incoherent IFSI is for the most part important in the region of $|y_1 - y'_1| \lesssim R_{int}$. In the variables $(x_1 - x'_1)$ and $(z_1 - z'_1)$ this interaction vanishes more slowly and survive at distances $\gtrsim R_{int}$ as well. Evidently, as in the case of $(e, e'p)$ reaction [10], the short range interaction between the two sets of the trajectories at the level of the Glauber absorptive factor will, for the most part, affect the missing momentum distribution at $p_m \gtrsim 1/R_{int} \sim 200$ MeV/c. However, on the contrary to $(e, e'p)$ reaction, in $(p, 2p)$ scattering due to the geometry of hard pp scattering, the azimuthal symmetry in the (x, y) plane is absent. The effect of the incoherent rescatterings must be enhanced in the region of large $p_{m,y}$ as compared with the cases of large $p_{m,x}$ or $p_{m,z}$.

The numerical calculations can be simplified exploiting the fact that in the integral

(21) $n_A(\vec{r})$ is a smooth function (in transverse directions) as compared to the profile functions. To factor out in (21) the transverse integration, we introduce a new coordinate system with the z -axis defined as a line which is the center of "gravity" of the trajectories $i_1, \dots, i_n, j_1, \dots, j_m$ in the (x, y) plane. Then, in terms of the new longitudinal, ξ , and transverse, $\vec{\tau}$, variables, to leading order in the small parameter R_{int}^2/R_A^2 (R_A is the nucleus radius) the integral (21) can be written as

$$G_{i_1, \dots, i_n}^{j_1, \dots, j_m}(\vec{r}_1, \vec{r}'_1) = \int d\xi n_A(0, 0, \xi) \theta(\vec{n}_\xi(\vec{r} - \vec{r}_1)) \dots \theta(\vec{n}_\xi(\vec{r} - \vec{r}'_1)) \theta(\vec{n}_\xi(\vec{r} - \vec{r}'_1)) \theta(\vec{n}_\xi(\vec{r} - \vec{r}'_1)) \\ \times \int d^2\vec{\tau} \Gamma_{i_1}(b_{i_1}(\vec{r}_1, \vec{\tau})) \dots \Gamma_{i_n}(b_{i_n}(\vec{r}_1, \vec{\tau})) \Gamma_{j_1}^*(b_{j_1}(\vec{r}'_1, \vec{\tau})) \dots \Gamma_{j_m}^*(b_{j_m}(\vec{r}'_1, \vec{\tau})). \quad (25)$$

Here we have written the nuclear density n_A as a function of the new variables, and the vector \vec{r} must be treated as a vector-function of ξ and $\vec{\tau}$. In Eq. (25) we have also taken advantage of the smallness of $\theta_{i.f.}$ and made replacements $\vec{n}_{i,j} \rightarrow \vec{n}_\xi$, where \vec{n}_ξ is the unit vector along ξ -axis. Evidently, similar to neglecting the simultaneous interaction of the spectator nucleon with the initial and final fast protons, such a replacement spoils the Glauber form of the attenuation factor only in a very narrow region of the spectator positions in the vicinity of the hard pp interaction vertex and practically does not affect the final numerical results. The integral over the transverse coordinates in Eq. (25) has the Gaussian form and can be calculated analytically. The corresponding formulas are somewhat lengthy and we do not present them here. The remaining integration over ξ was carried out numerically.

Eqs. (17), (20), (25) form the basis for evaluation of the missing momentum distribution ($p, 2p$) reaction within the Glauber model. Then, the nuclear transparency for a certain kinematical domain, D , of the missing momentum can be calculated through the formula

$$T_A(D) = \frac{\int_D d^3\vec{p}_m w(\vec{p}_m)}{\int_D d^3\vec{p}_m n_F(\vec{p}_m)}. \quad (26)$$

Besides the calculations of the nuclear transparency as a function of \vec{p}_m for the point-like domain D $T_A(\vec{p}_m) = w(\vec{p}_m)/n_F(\vec{p}_m)$, in the present paper we calculate the nuclear

transparency for the kinematical domains including all the values of the two and three components of the missing momentum. The one-dimensional missing momentum distributions obtained after the integration of $w(\vec{p}_m)$ over the two components of \vec{p}_m are given by

$$w_x(p_{m,x}) = \frac{1}{2\pi} \int dx dx' dy dz \rho(x, y, z, x', y, z) \Phi(x, y, z, x', y, z) \exp[i\vec{p}_{m,x}(x - x')], \quad (27)$$

$$w_y(p_{m,y}) = \frac{1}{2\pi} \int dx dy dy' dz \rho(x, y, z, x, y', z) \Phi(x, y, z, x, y', z) \exp[i\vec{p}_{m,y}(y - y')], \quad (28)$$

$$w_z(p_{m,z}) = \frac{1}{2\pi} \int dx dy dz dz' \rho(x, y, z, x, y, z') \Phi(x, y, z, x, y, z') \exp[i\vec{p}_{m,z}(z - z')], \quad (29)$$

The integrated nuclear transparency corresponding to the whole kinematical domain of the missing momentum in Eq. (26) is given by

$$T_A = \int d^3\vec{r}_1 \rho_A(\vec{r}_1) \Phi(\vec{r}_1, \vec{r}_1). \quad (30)$$

Making use of (20), (25) after a simple algebra we can represent (30) as

$$T_A = \int d^3\vec{r}_1 \rho_A(\vec{r}_1) \left\{ 1 - \frac{1}{A} \left[\sum_{i=1,3,4} \sigma_{in}^{pN}(E_i) t(\vec{r}_1, \vec{n}_i) - \delta(\vec{r}_1) \right] \right\}^{A-1}, \quad (31)$$

where

$$t(\vec{r}_1, \vec{n}_i) = \int_0^\infty dl n_A(\vec{r}_1 + \vec{n}_i l)$$

is the partial optical thickness function, and

$$\begin{aligned} \delta(\vec{r}_1) = & G_{34}(\vec{r}_1) + G^{34}(\vec{r}_1) + G_3^4(\vec{r}_1, \vec{r}_1) + G_4^3(\vec{r}_1, \vec{r}_1) + G_{34}^3(\vec{r}_1, \vec{r}_1) + G_{34}^4(\vec{r}_1, \vec{r}_1) \\ & + G_{34}^3(\vec{r}_1, \vec{r}_1) + G_{34}^4(\vec{r}_1, \vec{r}_1) + G_{34}^{34}(\vec{r}_1, \vec{r}_1). \end{aligned} \quad (32)$$

The terms containing the inelastic pN cross sections in the square brackets in the right-hand side of (31) describe the usual absorption in propagation of the fast protons in the nuclear medium, while $\delta(\vec{r}_1)$ yields correction for the shadowing in the final pp -system and the interference effects in the incoherent IFSI. Our numerical calculations show that this correction is non-negligible. Thus, even in the case of the integrated nuclear transparency,

the IFSI do not allow a probabilistic interpretation. However, it is worth noting, that the integrated nuclear transparency, as well as the transverse missing momentum distributions (27), (28), are not affected by the interference of amplitudes for rescatterings of the initial and final protons. One can see from Eq. (25) that the G -functions in the IFSI factor (20) related to this interference vanish for $z_1 = z_1'$.

Eq. (31) yields the nuclear transparency for the inclusive $(p, 2p)$ reaction. In the case of the exclusive reaction, after substituting in (30) the coherent IFSI factor (22), one can obtain for the integrated nuclear transparency

$$T_A^{exc} = \int d^3\vec{r}_1 \rho_A(\vec{r}_1) \left\{ 1 - \frac{1}{A} \left[\frac{1}{2} \sum_{i=1,3,4} \sigma_{tot}^{pN}(E_i) (1 - i\alpha_{pN}(E_i)) t(\vec{r}_1, \vec{n}_i) - G_{34}(\vec{r}_1) \right] \right\}^{A-1} \\ \times \left\{ 1 - \frac{1}{A} \left[\frac{1}{2} \sum_{i=1,3,4} \sigma_{tot}^{pN}(E_i) (1 + i\alpha_{pN}(E_i)) t(\vec{r}_1, \vec{n}_i) - G_{34}^*(\vec{r}_1) \right] \right\}^{A-1}. \quad (33)$$

We conclude this section with a short comment on the work [13] which previously considered $(p, 2p)$ scattering within the Glauber model. The authors of [13] also assume the factorization of hard pp scattering and soft IFSI, and use the factorized approximation (16) for the A -body semidiagonal density matrix. However, then they make use of the approximations which can not be justified. First, they neglect in their counterpart of our equation (17) the dependence of the IFSI factor on $\Delta\vec{r}_1 = (\vec{r}_1 - \vec{r}_1')$, and put $\vec{r}_1 = \vec{r}_1' = (\vec{r}_1 + \vec{r}_1')/2$. Under this approximation for the factorized parametrization of the one-body proton density matrix $\rho(\vec{r}, \vec{r}') = \rho_A(\frac{1}{2}(\vec{r} + \vec{r}'))W(\vec{r} - \vec{r}')$ (here $W(\vec{r} - \vec{r}')$ is the Fourier transform of the SPMD) they obtained the missing momentum distribution which is proportional to the SPMD. Evidently, the approach of ref. [13] misses all the distortion effects which, as we shall demonstrate below, are quite strong. Our predictions for the integrated nuclear transparency also differ from the results of ref. [13], because in the analysis [13] the shadowing in the final pp -system and interference effects in the incoherent IFSI were not taken into account.

III. NUMERICAL RESULTS

In this section we present our numerical results based on the formalism developed in the previous section. We performed the calculations for the target nuclei ^{12}C , ^{16}O , ^{27}Al and ^{40}Ca . For ^{12}C and ^{27}Al we compare the numerical results with the available data of the BNL experiment [6,17]. The calculations were performed for the oscillator shell wave functions. We adjusted the oscillator frequency, ω_{osc} , for the above set of the nuclei to reproduce the experimental values of the root-mean-square radius of the charge distribution: $\langle r^2 \rangle^{1/2} = 2.47, 2.73, 3.05$ and 3.47 fm for ^{12}C , ^{16}O , ^{27}Al and ^{40}Ca [19], respectively. We obtained the following set of the values of the oscillator radius $r_{osc} = (m_p \omega_{osc})^{-1/2} = 1.59, 1.74, 1.78$ and 1.95 fm. The difference between the charge distribution and the proton nuclear density connected with the proton charge radius was taken into account. The charge density and SPMD in the region of $p_m \lesssim 300$ Mev/c, calculated with the above set of the oscillator radii are practically indistinguishable from the results of more involved Hartree-Fock calculations. The SPMD calculated in the harmonic oscillator shell model is also close to the one obtained within a many-body approach with realistic nucleon-nucleon potential in ref. [20].

As it was stated in section 2, we use the exponential parameterization of the proton-nucleon elastic amplitude. The diffraction slope of the pN scattering was estimated from the relation

$$B_{pN} \approx \frac{\sigma_{tot}^2(pN)(1 + \alpha_{pN}^2)}{16\pi\sigma_{el}(pN)}. \quad (34)$$

In our calculations we define the pN cross sections and α_{pN} as mean values of these quantities for the pp and pn scattering. We borrowed the experimental data on pp , pn cross sections and α_{pp} , α_{pn} from the recent review [21].

In Figs. 1, 2 and 3 we show the nuclear transparency for $^{16}\text{O}(p, 2p)$ and $^{40}\text{Ca}(p, 2p)$ reactions at $p_{lab} = 6$ and 12 GeV/c (here $p_{lab} = p_1$ is the incident beam momentum) as function of \vec{p}_m for the two transverse and the longitudinal directions of the missing momentum, respectively. Besides the results for the whole IFSI factor (20) (solid curve)

corresponding to the inclusive reaction, we also show the results for the exclusive reaction obtained with the coherent IFSI factor (22) (dashed curve). To illustrate the role of the interference and shadowing effects in the incoherent IFSI we present in Fig. 1-3 the results obtained keeping in the square brackets in the right-hand side of Eq. (20) only the terms G_i , G^i and the diagonal second order terms G_i^i (dot-dashed curve). In Figs. 1-3 we also show the nuclear transparency for the exclusive reaction obtained neglecting the shadowing term G_{34} in (23). Figs. 1-3 demonstrate that the IFSI-distortion effects are strong both for the inclusive and exclusive reactions. It is seen that the increase of p_{lab} from 6 up to 12 GeV/c practically does not change the nuclear transparency. However, as one can see the \vec{p}_m -dependence of the nuclear transparency appears to be sensitive to the shell structure of the target nucleus. Figs. 1, 2 show that for the both transverse directions of the missing momentum the incoherent IFSI become very important at $p_{m\perp} \gtrsim 150 - 200$ MeV/c. In the case of the parallel kinematics the difference between the nuclear transparencies for the inclusive and exclusive reactions is relatively small at $|p_{m,z}| \lesssim 200$ MeV/c. The results presented in Figs. 1-3 indicate that in the case of $(p, 2p)$ reaction in the region of $p_m \lesssim 100 - 150$ MeV/c the incoherent IFSI increase the nuclear transparency by 5-10%. The Glauber analysis of $(e, e'p)$ reaction [10] yields the relative effect of the incoherent rescatterings $\lesssim 3\%$ in this region of the missing momentum. Thus, we see that the transition from $(e, e'p)$ to $(p, 2p)$ reaction enhances the effect of the incoherent rescatterings substantially. None the less our analysis indicates that the optical approach which neglects the incoherent rescattering is a reasonable starting point for qualitative evaluation of the nuclear transparency in $(p, 2p)$ reaction for the relatively small missing momenta ($p_m \lesssim 100 - 150$ MeV/c). This fact is of great importance for the prospect of the further study of CT effects in this reaction. From this point of view it is also important that, as one can see from Figs. 1-3, the shadowing correction also does not affect the nuclear transparency for exclusive reaction considerably, and can be neglected in the above region of the missing momentum. Notice, that Figs. 1-3 demonstrate that neglecting the shadowing and interference effects in the incoherent IFSI leads to a considerable

underestimate of the contribution of the incoherent rescatterings.

In Figs. 4-6 we present the nuclear transparency calculated for the kinematical domains including all the values of the two components of the missing momentum. The legend of the curves is the same as in Figs. 1-3. It is seen that the integration over the two components of the missing momentum enhances the relative effect of the incoherent IFSI as compared with the unintegrated nuclear transparency. The contribution of the incoherent rescatterings becomes important even in the case of the $p_{m,z}$ -dependence of T_A .

The results for the integrated nuclear transparency obtained for the same versions of the IFSI factors as in Figs. 1-6 are presented in Fig. 7. Fig. 7 further demonstrates that neglecting the shadowing and interference terms leads to the underestimate of the contribution of the incoherent rescatterings in the inclusive $(p, 2p)$ scattering by the factor ~ 2 . In the case of the exclusive reaction the shadowing in the final pp -system gives rise to the increase of T_A by $\sim 10\%$.

The curves shown in Fig. 6 were obtained according to the formula (26). In ref. [6] the $p_{m,z}$ -dependence of the nuclear transparency were extracted from the cross section of $(p, 2p)$ scattering making use of for the one-dimensional SPMD the experimentally measured $p_{m,y}$ -distribution (after its normalization to unity). For this reason the data of [6] must be compared with the theoretical nuclear transparency defined as

$$T_A^{BNL}(p_{m,z}) = \frac{w_z(p_{m,z})}{w_y^{norm}(p_{m,z})}, \quad (35)$$

where

$$w_y^{norm}(p) = \frac{w_y(p)}{T_A} \quad (36)$$

is the normalized to unity one-dimensional IFSI-distorted $p_{m,y}$ -distribution. The comparison of the theoretically calculated ratio (36) for the whole IFSI factor (20) with the experimental data of ref. [6] for $^{27}\text{Al}(p, 2p)$ scattering is presented in Fig. 8. As one can see, the predictions of the Glauber model are in good agreement with the data [6] at

$p_{lab} = 6$ GeV/c. Notice, that the fall down of the theoretically calculated nuclear transparency with increase of $|p_{m,z}|$ is a consequence of the above mentioned enhancement of the contribution of the incoherent rescatterings in the region of large $|p_{m,y}|$ as compared with the case of large $|p_{m,z}|$. At $p_{lab} = 10$ the experimental values of the transparency in the region of $p_{m,z} > 0$ are in excess of the theoretical curve by the factor ~ 2 . At $p_{lab} = 12$ GeV/c only one experimental point (the bin $200 < p_{m,z} < 300$ MeV/c) overshoots the Glauber curve.

In Fig. 9 we compare the theoretical $p_{m,y}$ -distribution (36) with the BNL experimental data [17] for $^{12}C(p, 2p)$ and $^{27}Al(p, 2p)$ reaction at $p_{lab} = 6$ and 10 GeV/c. Besides the predictions obtained with the whole IFSI factor (solid curve) we show the distribution for the exclusive reaction and the one-dimensional SPMD. As one can see the exclusive distribution and SPMD differ drastically from the experimental distribution. The theoretical distribution obtained with the whole IFSI factor is in good agreement with experimental data for both nuclei at $p_{lab} = 6$ GeV/c. However, at $p_{lab} = 10$ GeV/c for $^{27}Al(p, 2p)$ reaction the width of the experimental distribution is in excess of the width of the theoretical distribution. In all probability the disagreements of the Glauber model predictions in the cases of the $p_{m,z}$ -dependence of the nuclear transparency, Fig.8, and the $p_{m,y}$ -distribution, Fig.9, with the data of ref. [6,17] for $^{27}Al(p, 2p)$ reaction at $p_{lab} = 10$ GeV/c are caused by the same reason.

IV. CONCLUSIONS

The purpose of this work has been a study of IFSI effects in hard $(p, 2p)$ scattering in the region of moderate missing momenta $|\vec{p}_m| \lesssim 300$ MeV/c within the Glauber model. To perform such an analysis, we generalized the Glauber theory developed for the small-angle hadron-nucleus collisions at high energy, to the case of hard $(p, 2p)$ reaction. We studied the missing momentum dependence of IFSI effects both for inclusive and exclusive $(p, 2p)$ scattering. The analysis was performed taking into account the shadowing and interference effects in IFSI which were not discussed previously.

Our numerical results show that the missing momentum distribution in $(p, 2p)$ reaction is substantially affected by IFSI as compared to the PWIA case both for the inclusive and exclusive conditions. In the inclusive $(p, 2p)$ scattering the incoherent IFSI become dominant at $p_{m\perp} \gtrsim 150 - 200$ MeV/c. Our results show that neglecting the shadowing and the interference effects leads to considerable underestimation of the contribution of the incoherent rescatterings. In the region of $p_m \lesssim 100 - 150$ MeV/c the incoherent IFSI increase the missing momentum distribution only by 5-10%. Therefore, at the relatively small missing momenta the optical approach is still applicable for a qualitative evaluation of IFSI effects. This fact is of great importance for the further investigations of CT effects in $(p, 2p)$ reactions because neglecting the incoherent rescatterings simplifies the calculations within the coupled-channel approach considerably. Our results also indicate that in future experiments it is highly desirable to measure the nuclear transparency separately for the regions of small ($p_m \lesssim 150$ MeV/c) and high ($p_m \gtrsim 200$ MeV/c) missing momenta.

For the first time nuclear transparency measured in the BNL experiment [6] has been compared with the theoretically calculated transparency defined according to the prescription of ref. [6]. We emphasize that for the strong distortions of $W_y(p_{m,y}), W_z(p_{m,z})$ and the strong dependence of $T_A^{BNL}(p_{m,z})$ on $p_{m,z}$ at fixed beam momentum p_{lab} , it does not make any sense to plot T_A^{BNL} vs. $p_{lab}^{eff} = p_{lab}(1 - \frac{p_{m,z}}{m_p})$ and it is erroneous to interpret the so obtained p_{lab}^{eff} dependence of T_A^{BNL} as the true energy dependence of nuclear transparency. We also compared the predictions of the Glauber model with the $p_{m,y}$ -distribution observed in the BNL experiment [17], such a comparison has also been performed for the first time. In both cases a good agreement of the Glauber model predictions with experiment was found at $p_{lab} = 6$ GeV/c. However, the predictions of the Glauber model disagree with the data of refs. [6,17] at $p_{lab} = 10$ GeV/c. Our analysis indicates that the discrepancy between the Glauber model results for nuclear transparency and the $p_{m,y}$ -distribution and the data from the BNL experiment at $p_{lab} = 10$ GeV/c are likely to be connected with the same cause.

Finally it is appropriate to comment on the status of predictions of the one-channel Glauber model and on the role of the off-diagonal rescatterings in the GeV's energy region. There is a widespread opinion that contribution of the off-diagonal rescatterings vanishes at the energies much smaller than the CT energy scale $E_{CT} \sim R_A(m_p^{*2} - m_p^2)/2 \sim 10 - 20$ GeV (here m_p^* is the mass of the radial excitation of the proton). Our recent analysis [12] demonstrates that in the case of $(e, e'p)$ and $(p, 2p)$ reactions this is only the case for the coherent rescatterings, while the contribution of the incoherent off-diagonal rescatterings becomes small only at the energy of the fast proton(s) $E_p \lesssim E_{inc} \sim \Gamma_{p^*} m_{p^*} l_{int} \sim 2 - 3$ GeV (here $l_{int} \sim (\sigma_{tot}(pN)\langle n_A \rangle)^{-1}$ is the mean free path of the proton in the nuclear medium, Γ_{p^*} is the width of the resonant state). At higher energies ($\gtrsim E_{CT}$) the off-diagonal rescatterings increase the nuclear transparency for the coherent rescatterings and decrease it for the incoherent rescatterings. Such an interplay of the coherent and incoherent IFSI can lead to an irregular energy dependence of the nuclear transparency in inclusive $(p, 2p)$ reaction in the energy region of the BNL experiment. The analysis of ref. [12] shows that for $(e, e'p)$ reaction the off-diagonal rescatterings may enhance the contribution of the incoherent rescatterings by the factor ~ 2 in the energy region of the final proton $E_{inc} \lesssim E_p \lesssim E_{CT}$. In the case of $(p, 2p)$ reaction the enhancement factor must be ~ 4 . Consequently, the off-diagonal incoherent rescatterings may increase the nuclear transparency in $(p, 2p)$ reaction at $p_{lab} \sim 10$ GeV/c by the factor ~ 2 . Notice, that correlation of the increase of nuclear transparency with the broadening of $p_{m,y}$ -distribution observed in [6,17] in $^{27}Al(p, 2p)$ reaction at $p_{lab} = 10$ GeV/c gives evidence in favor of the off-diagonal incoherent rescatterings as a cause of the above rise of nuclear transparency. The above estimate corresponds to the off-diagonal rescatterings with the color-singlet intermediate $3q$ states, and here it is appropriate to comment on the possible contribution from the hidden-color intermediate states. Namely, at high energies the scattering angle in the laboratory frame $\theta_{l.f.} \ll 1$, and the two $3q$ states produced in hard pp collision can interact with the same spectator nucleon. For this reason the new kind of the hidden-color (for instance the $(3q)_{\{8\}}(3q)_{\{8\}}$ state) intermediate states of the two final $3q$ states produced

in hard pp collision may come into play. In the case of the production of the $(3q)_{\{8\}}(3q)_{\{8\}}$ state the intermediate hidden-color state can undergo the transition to the normal $(3q)(3q)$ state after rescattering on the spectator nucleon $(3q)_{\{8\}}(3q)_{\{8\}} + N \rightarrow (3q)_{\{1\}}(3q)_{\{1\}} + N$. It is important that in contrary to the discussed in the present paper shadowing effect in the final pp system, the transition of the hidden-color $(3q)_{\{8\}}(3q)_{\{8\}}$ state into the normal $(3q)(3q)$ state requires only one Pomeron exchange. Of course, the production amplitude for the hidden-color states will be suppressed by the Sudakov form factor. However, in the GeV's energy region this mechanism may be potentially important due to the enhancement by the factor $\sim N_c^2$ as compared with the production of the normal $(3q)(3q)$ states in hard pp interaction. Thus, we see that one can expect a complicated interplay of the diagonal and off-diagonal rescatterings in $(p, 2p)$ reaction in GeV's energy region. For this reason, we regard the predictions of the Glauber model only as a baseline which allows us to understand the gross features of the coherent and incoherent IFSI and can help in further investigation of CT effects in $(p, 2p)$ reaction.

ACKNOWLEDGMENTS

This work was partly supported by the Grant N9S000 from the International Science Foundation and the INTAS grant 93-239. AAU acknowledges Prof. A. Zichichi and ICSC- World Laboratory for financial support. BGZ wishes to gratefully acknowledge the hospitality of the Interdisciplinary Laboratory of SISSA and the Institut für Kernphysik, KFA, Jülich.

REFERENCES

- [1] A.H.Mueller, *in: Proceedings of the XVII Rencontre de Moriond, Les Arcs, France.* Ed. Trinh Thanh Van, Editions Frontieres, Gif-sur-Yvette, 1982, p.13.
- [2] S.J.Brodsky, *in: Proceedings of the XIII International Symposium on Multiparticle Dynamics, Volendam, Netherlands.* Eds. E.W.Kittel, W.Metzger and A.Stergion, World Scientific, Singapore, 1982, p. 963.
- [3] R.J.Glauber, *in: Lectures in Theoretical Physics*, v.1, ed. W.Brittain and L.G.Dunham. Interscience Publ., N.Y., 1959; R.J.Glauber and G.Matthiae, *Nucl. Phys.* **B21** (1970) 135.
- [4] V.N.Gribov, *Sov. Phys. JETP* **29** (1969) 483; **30** (1970) 709.
- [5] S.J.Brodsky and G.P.Lepage, *Phys. Rev.* **D22** (1980) 2157.
- [6] A.S.Carroll et al., *Phys.Rev.Lett.* **61** (1988) 1698.
- [7] S.J.Brodsky and G.F. de Teramond, *Phys.Rev.Lett.* **60** (1988) 1924.
- [8] J.Ralston and B.Pire, *Phys. Rev. Lett.* **61** (1988) 1823.
- [9] B.Z.Kopeliovich and B.G.Zakharov, *Phys.Lett.* **B264** (1991) 434.
- [10] N.N.Nikolaev, J.Speth, B.G.Zakharov, Jülich preprint **KFA-IKP(Th)-1995-01**, January 1995, *J. Exp. Theor. Phys.* (1996) in print.
- [11] J.Nemchik, N.N.Nikolaev and B.G.Zakharov, *Proceedings of the Workshop on CEBAF at Higher Energies, CEBAF, April 14-16, 1994*, Editors: Nathan Isgur and Paul Stoler, pp. 415-464.
- [12] O.Benhar, S.Fantoni, N.N.Nikolaev, J.Speth, A.A.Usmani and B.G.Zakharov, submitted to *Z. Phys.* **A**.
- [13] A.Kohama, K.Yazaki and R.Seki, *Nucl.Phys.* A536 (1992) 716.

- [14] J.W.Van Orden, W.Truxex and M.K.Banerjee, *Phys. Rev.* **C21** (1980) 2628; S.Fantoni and V.R.Pandharipande, *Nucl. Phys.* **A427** (1984) 473; S.C.Pieper, R.B.Wiringa and V.R.Pandharipande, *Phys. Rev. C46* (1992) 1741.
- [15] A.Bianconi, S.Jeschonnek, N.N.Nikolaev and B.G.Zakharov, *Phys.Lett.* **B343** (1995) 13.
- [16] A.Bianconi, S.Jeschonnek, N.N.Nikolaev and B.G.Zakharov, Jülich preprint **KFA-IKP(Th)-1995-13**, March 1995, submitted to *Nucl. Phys. A*.
- [17] S.Heppelmann et al., *Phys. Lett.* **B232** (1989) 167.
- [18] G.D.Alkhozov, S.I.Belostotsky and A.A.Vorobyev, *Phys. Rep.* **C42** (1978) 89.
- [19] H. de Vries et al., *Atomic Data and Nuclear Data Tables* **36** (1987) 496
- [20] O.Benhar, C.Ciofi Degli Atti, S.Liuti and G.Salme, *Phys. Lett.***B177** (1986) 135.
- [21] C.Lechanoine-LeLuc and F.Lehar, *Rev.Mod.Phys.* **65** (1993) 47.

Figure captions:

- Fig. 1 - The $p_{m,x}$ -dependence of nuclear transparency for $^{16}\text{O}(p, 2p)$ and $^{40}\text{Ca}(p, 2p)$ scattering at $p_{m,y} = p_{m,z} = 0$. The solid curve is for the inclusive reaction, the dashed curve is for the exclusive reaction, the dot-dashed curve shows the results obtained keeping in the IFSI factor (20) only the terms G_i , G^i and G_i^i , the dotted curve corresponds to the IFSI factor (22) without the shadowing term G_{34} in (23).
- Fig. 2 - The same as Fig. 1, but for the $p_{m,y}$ -dependence of nuclear transparency at $p_{m,z} = p_{m,x} = 0$.
- Fig. 3 - The same as Fig. 1, but for the $p_{m,z}$ -dependence of nuclear transparency at $p_{m,x} = p_{m,y} = 0$.
- Fig. 4 - The $p_{m,x}$ -dependence of nuclear transparency integrated over $p_{m,y}$ and $p_{m,z}$. The legend of the curves is the same as in Figs. 1-3.
- Fig. 5 - The $p_{m,y}$ -dependence of nuclear transparency integrated over $p_{m,z}$ and $p_{m,x}$. The legend of the curves is the same as in Figs. 1-3.
- Fig. 6 - The $p_{m,z}$ -dependence of nuclear transparency integrated over $p_{m,x}$ and $p_{m,y}$. The legend of the curves is the same as in Figs. 1-3.
- Fig. 7 - Integrated nuclear transparency for $^{12}\text{C}(p, 2p)$, $^{16}\text{O}(p, 2p)$, $^{27}\text{Al}(p, 2p)$ and $^{40}\text{Ca}(p, 2p)$ reactions. The legend of the curves is the same as in Figs. 1-3.
- Fig. 8 - Comparison of the Glauber model predictions for $p_{m,z}$ -dependence of nuclear transparency defined according to Eq. (35) with the experimental data of ref. [6] for $^{27}\text{Al}(p, 2p)$ reaction.
- Fig. 9 - The $p_{m,y}$ -dependence of the one-dimensional normalized to unity missing momentum distribution in $^{12}\text{C}(p, 2p)$ and $^{27}\text{Al}(p, 2p)$ reactions. The solid curve is for the Glauber model predictions for the whole IFSI factor (20), the dashed curve shows the predictions of the Glauber model obtained with the coherent IFSI factor (22),

the dotted curve shows SPMD, the histogram shows the experimental distribution observed in [17].

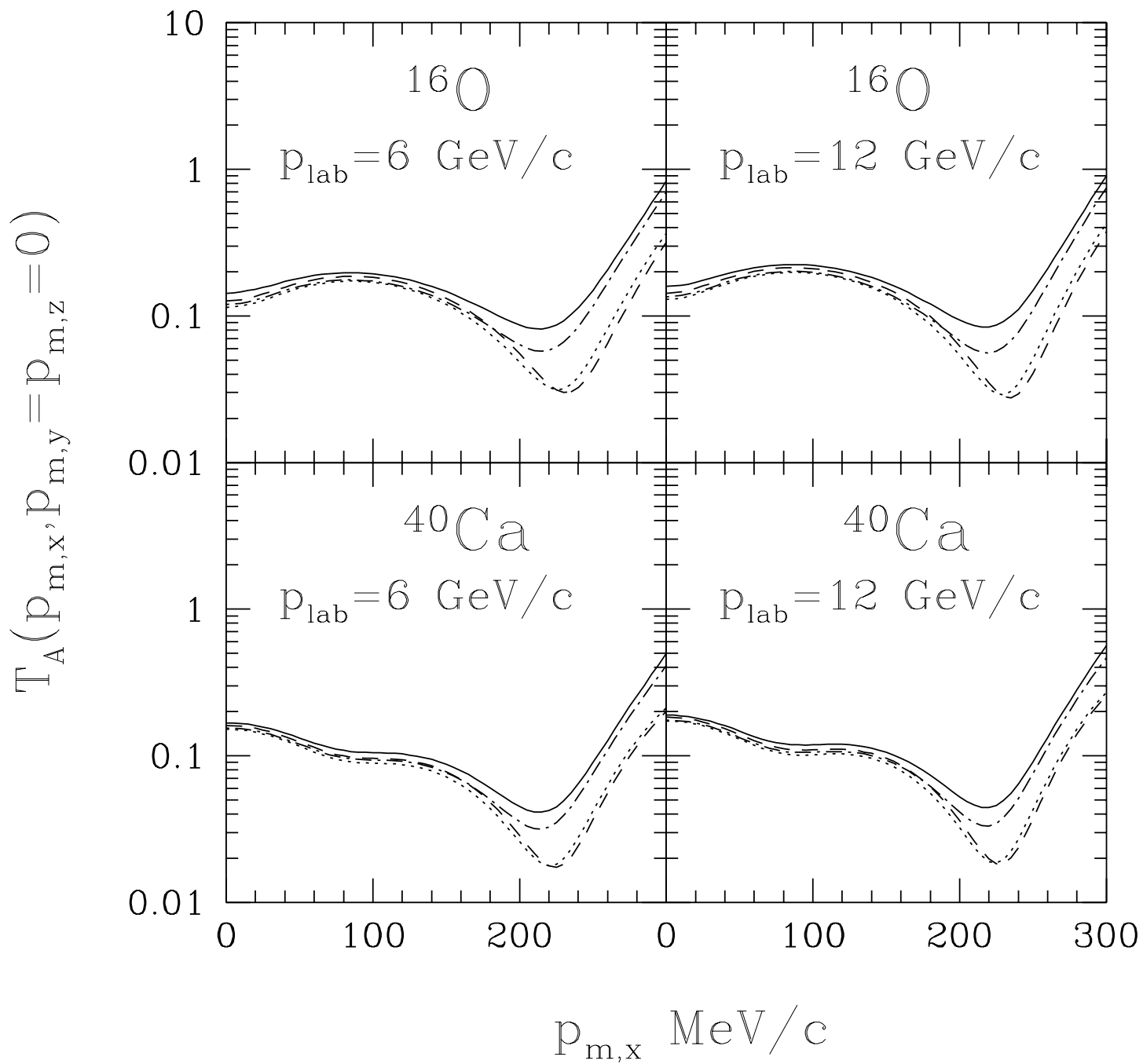


fig1. (p,2p)

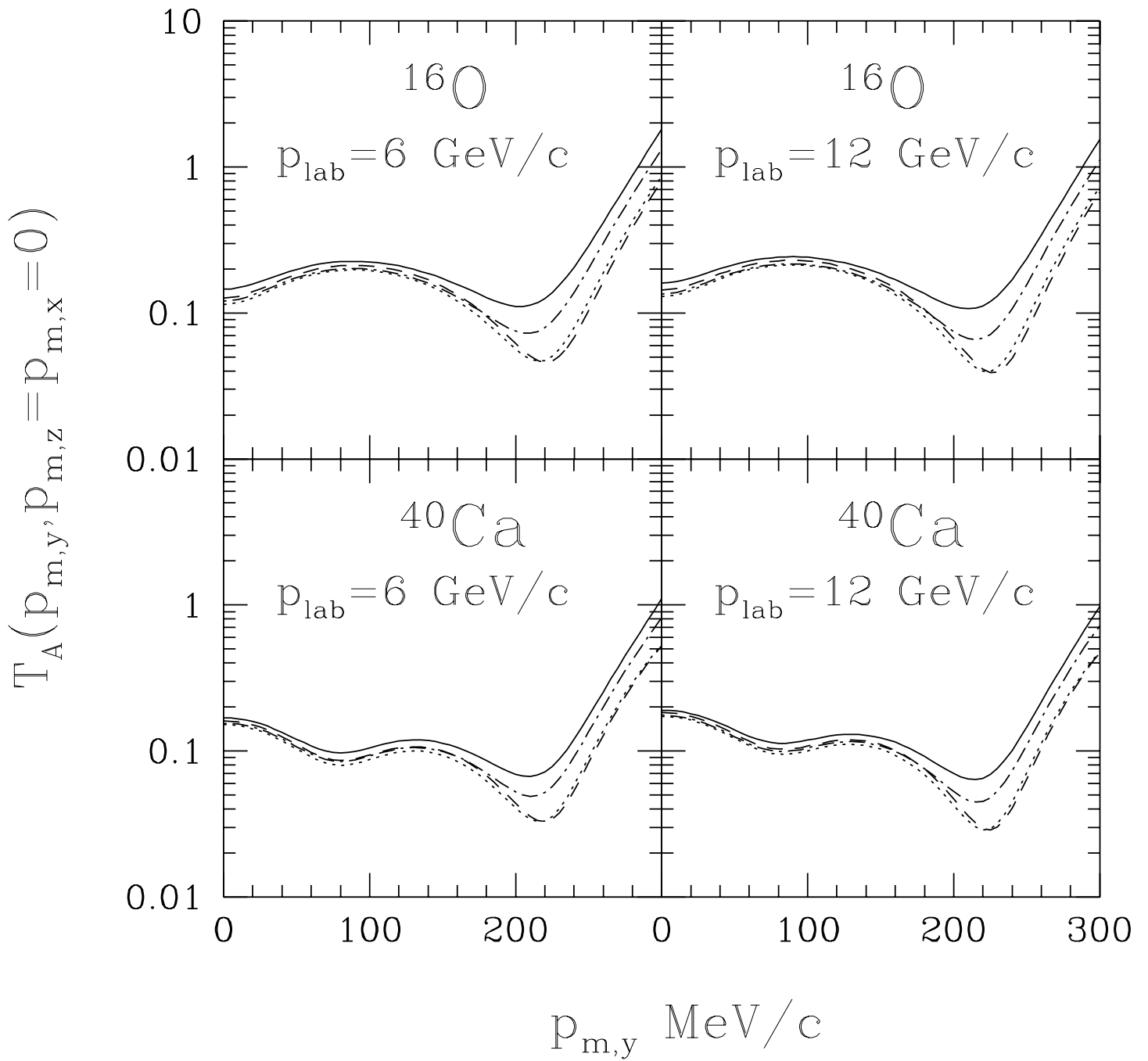


fig2. (p,2p)

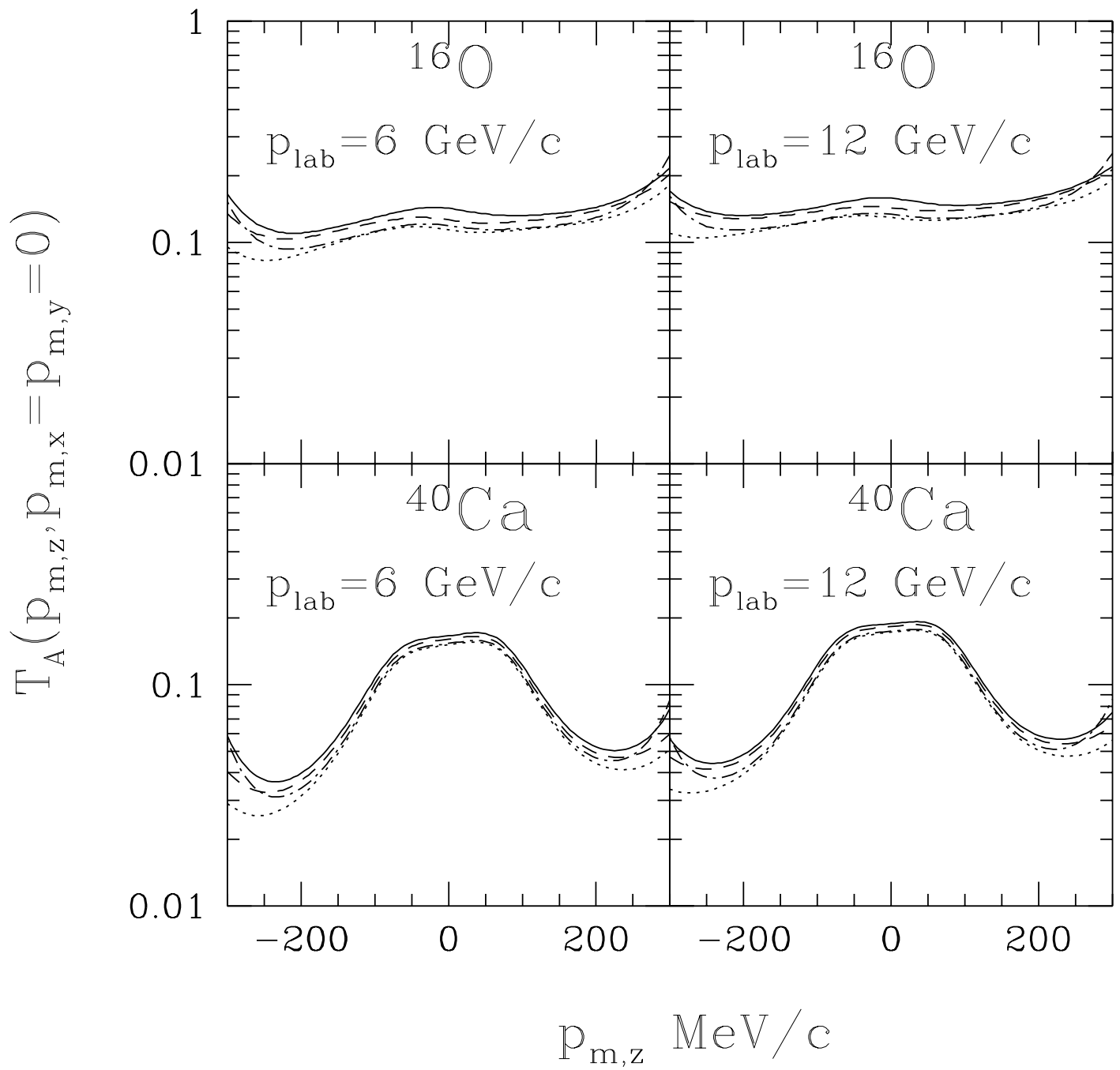


fig3. (p,2p)

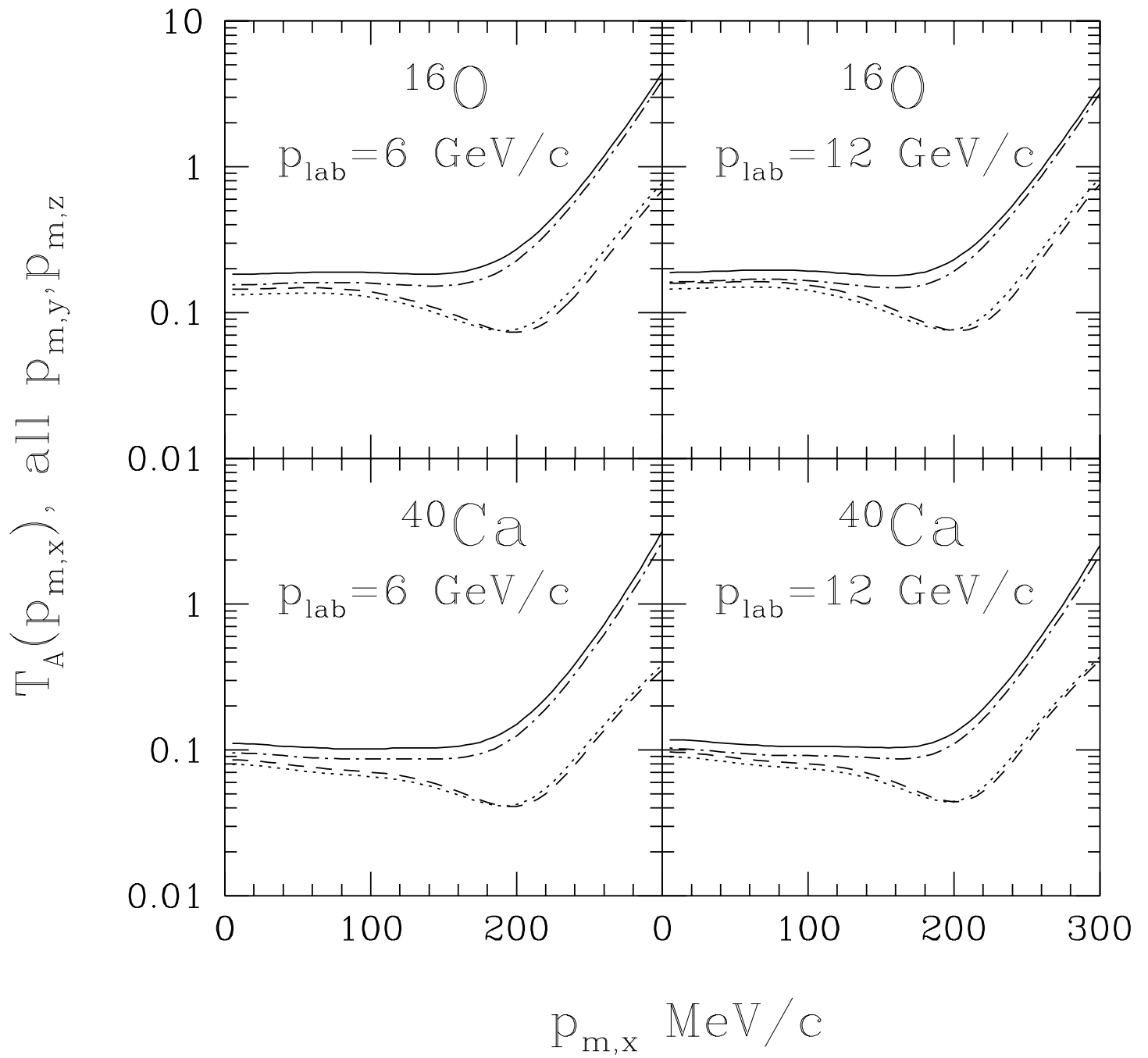


fig4. (p,2p)

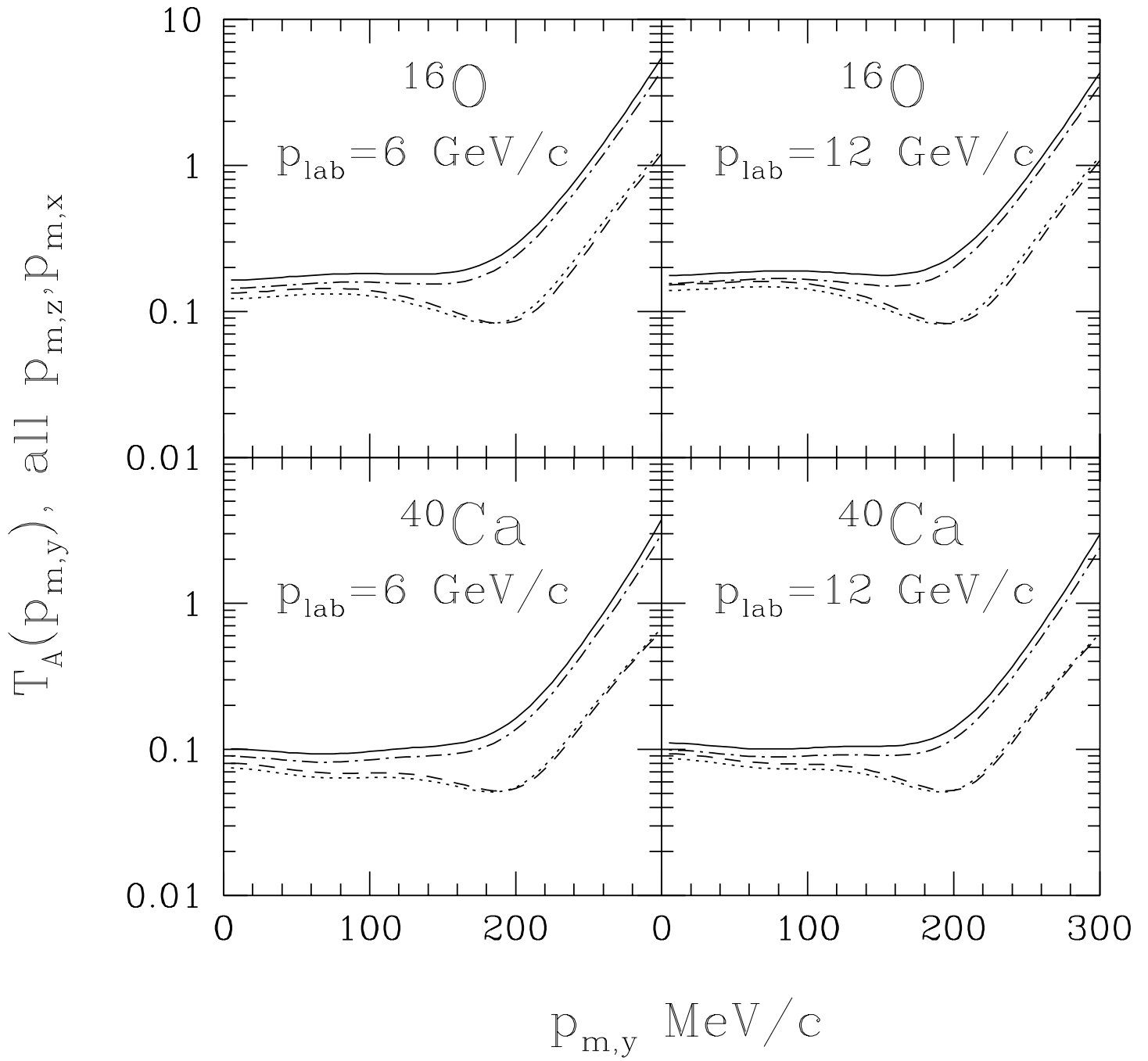


fig5. (p,2p)

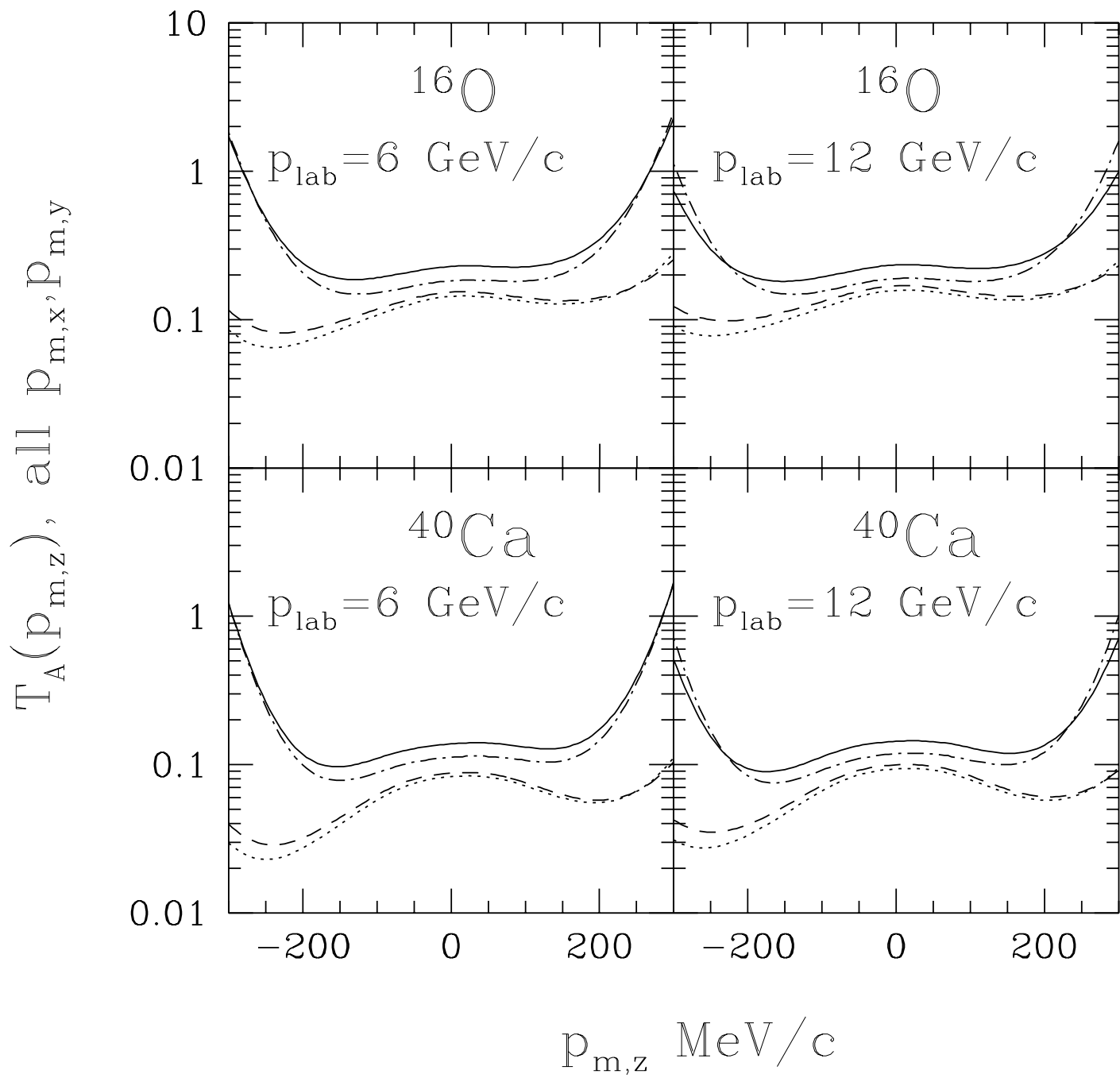


fig6. (p,2p)

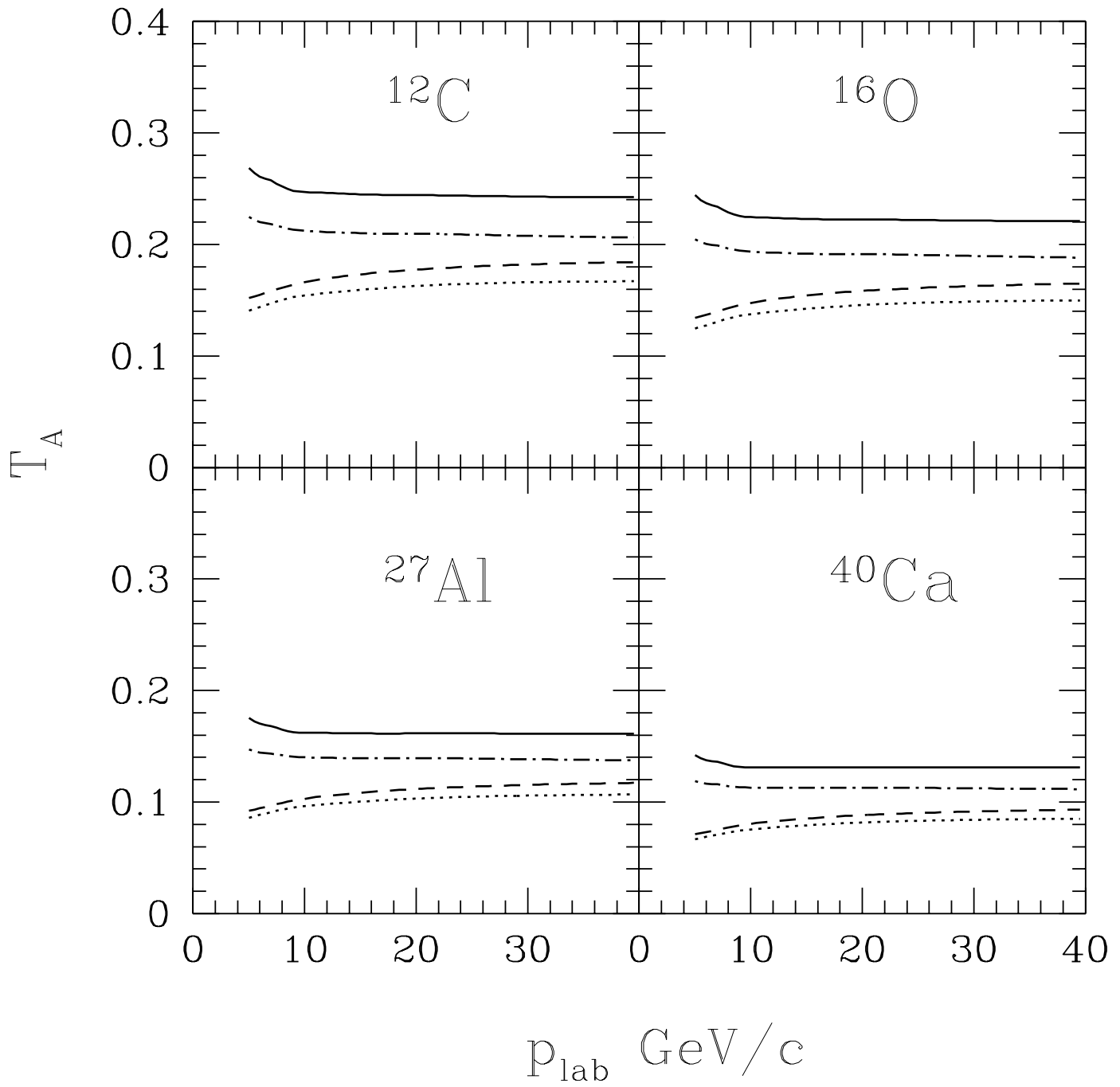


fig7. (p,2p)

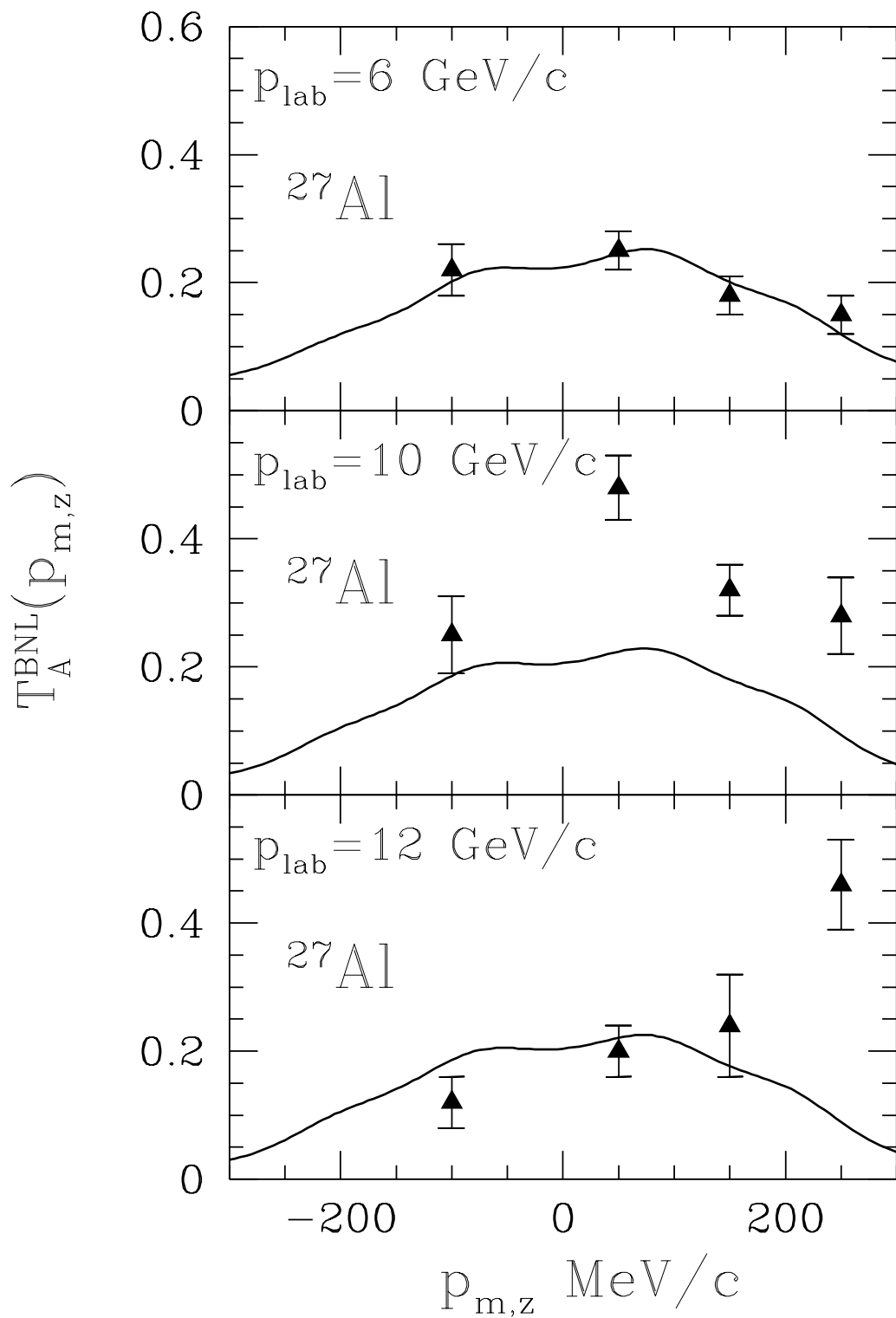


fig8. (p,2p)

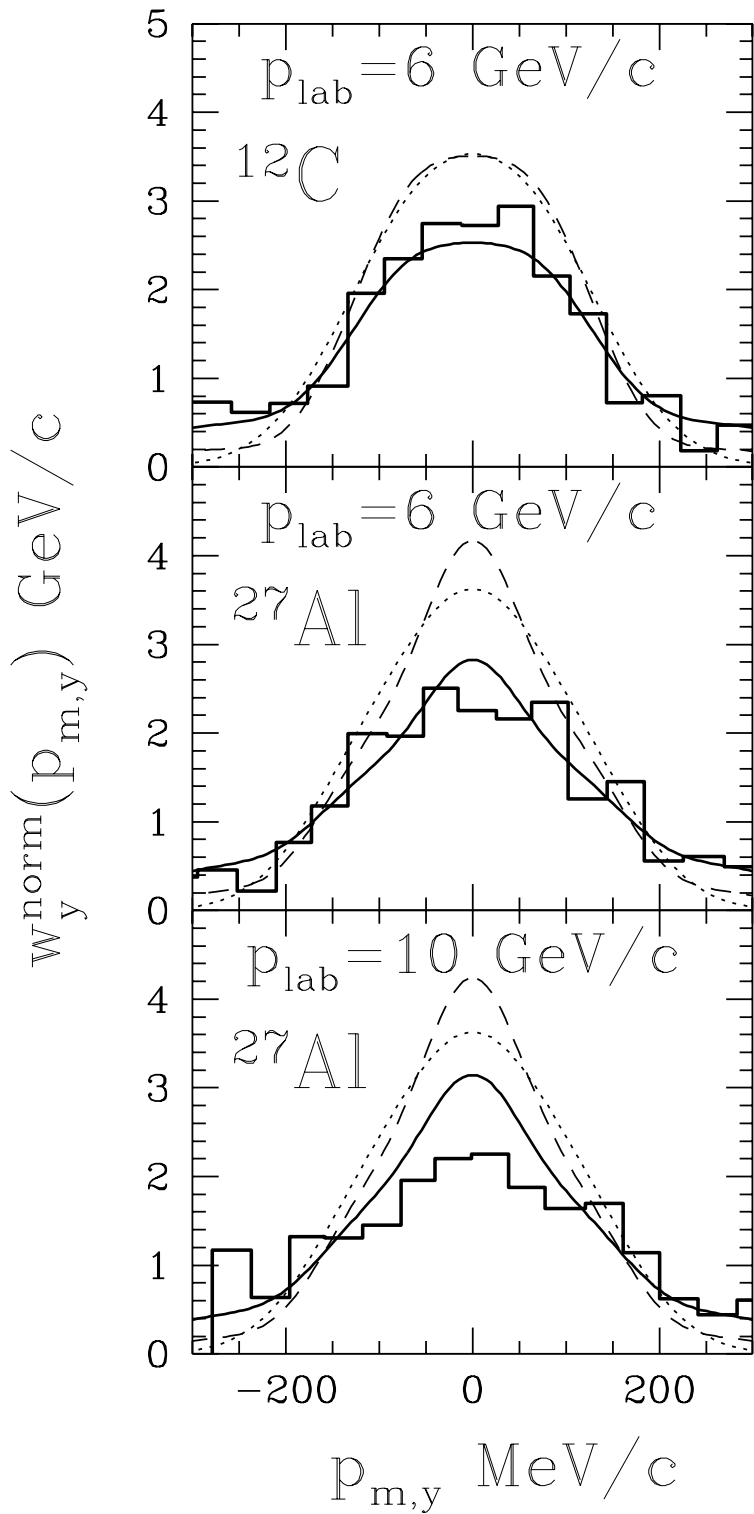


fig9. (p,2p)